



Article

The Influence of Alkaline Pretreatment of Waste Nutshell for Use in Particulate Biocomposites

Filip Brleković *, Katarina Mužina and Stanislav Kurajica

Faculty of Chemical Engineering and Technology, University of Zagreb, Marulićev Trg 19, 10000 Zagreb, Croatia; kmuzina@fkit.unizg.hr (K.M.); stankok@fkit.unizg.hr (S.K.)

* Correspondence: fbrlekovi@fkit.unizg.hr

Abstract: The aim of this work was to determine how different types of alkaline pretreatment influence the properties of waste almond and hazelnut nutshell, as well as their compatibility with model inorganic geopolymer matrixes for the formation of biocomposites with potential use in civil engineering. For alkaline pretreatment, 3, 6 and 9% NaOH water solutions and milk of lime were used under different temperature and time conditions. The rise in the crystallinity index was confirmed by X-ray powder diffraction analysis, while the corroboration of the removal of amorphous and undesirable components was demonstrated through Fourier-transform infrared spectroscopy. Furthermore, the effectiveness of the pretreatments was confirmed via simultaneous differential thermal and thermogravimetric analysis, and the positive change in the morphology of the surface of the waste nutshell (WN) and the deposition of the desired phases was established using scanning electron microscopy. Surface free energy and adhesion parameters were calculated using the Owens, Wendt, Rabel and Kaelble method for WN as fillers and geopolymers as model novel inorganic binders. This research indicates that the 6% NaOH treatment is the optimal pretreatment process for preparing WN as the filler in combination with potassium and metakaolin geopolymer that has been cured at room temperature.

Keywords: biocomposites; waste nutshell; mercerization; lignocellulosic materials



Citation: Brleković, F.; Mužina, K.; Kurajica, S. The Influence of Alkaline Pretreatment of Waste Nutshell for Use in Particulate Biocomposites. *J. Compos. Sci.* **2024**, *8*, 26. <https://doi.org/10.3390/jcs8010026>

Academic Editors: Francesco Tornabene and Thanasis Triantafyllou

Received: 20 November 2023

Revised: 14 December 2023

Accepted: 2 January 2024

Published: 11 January 2024



Copyright: © 2024 by the authors. Licensee MDPI, Basel, Switzerland. This article is an open access article distributed under the terms and conditions of the Creative Commons Attribution (CC BY) license (<https://creativecommons.org/licenses/by/4.0/>).

1. Introduction

Agriculture, as one of the fundamental human activities, produces high amounts of waste material. Large portions of these waste materials are not managed or disposed of properly. This problem is particularly present in less-developed countries, whose economies predominantly rest on agricultural production and produce export. Rough estimates are that 1.3 billion tonnes of agricultural waste are generated annually [1], which calls for the development of new agricultural waste utilization technologies. Such technologies that rely on the utilization of agricultural waste could yield new materials with added value [2]. Among the types of agricultural waste, different lignocellulosic materials such as nutshells are generated in great quantities. WN is routinely used as a fuel due to its calorific value, which is comparable to wood biomass. This type of waste management is not in accordance with the objectives of the progressive and environmentally friendly policies and circular economy. Consequently, new possibilities and applications for these kinds of materials are being researched and developed, with one of the prominent applications being their use as a filler material for biocomposites in construction industry or as a bioadsorbent [3]. Almond and hazelnut belong to the group of nuts with the highest production demand due to high human consumption. Furthermore, up to 50% of the nut product is the WN, which belongs to the lignocellulosic group of materials (LCM). Typical almond nutshell comprises 50% cellulose, 28% hemicellulose and 20% lignin, while the hazelnut shell has a comparable composition with 35% hemicellulose and 32% lignin but lower values for cellulose, commonly around 30%, [4]. The composition of both nutshells depends on

the climate, soil and other growth conditions. Alongside these primary components, the amount of extractable sugar, fat, wax and pectin is similar in both nutshells and does not exceed 4% [5–7]. High potassium content interferes with the use of waste almond shells as fuel, particularly if high temperatures are reached, due to possible furnace corrosion and clogging [8,9]. Different traditional and advanced applications for almond shell are being researched, for example, as a precursor to biochars used in the adsorption of pollutants and pharmaceuticals, a biogas, bio-oils or in the production of bioethanol [10]. Crushed and milled almond shell is used as a filler, mechanical property modifier and colorant in different composites with polymethyl methacrylate, polylactide, polypropylene and various epoxy resins as polymer matrix [11]. Similar to the almond shell, the hazelnut shell is also used as a bioadsorbent due to the presence of various organic groups on the shell surface, as well as its beneficial micro- and mesoporous structure, which allows for the effective removal of heavy metals in addition to different organic pollutants [12]. The hazelnut shell shows a promising future as a natural source of different phenolic antioxidants and as a filler in inorganic and organic composite materials. Particle boards made of hazelnut shell with organic resins as binders are already being produced, while inorganic matrix composites are based mostly on the preparation of lightweight bricks in which the nutshell fillers are burned during the firing of the bricks, which allows for the formation of a highly porous structure [13–15].

One of the possible uses of WN is in the production of inorganic insulating composites used in civil engineering. Natural fillers such as waste nutshell in those composites enable the achievement of eco-friendly and advanced properties. Additionally, in this manner, the CO₂ used for the plant's growth is "trapped" in the composite material in contrast to being released during the firing of the nutshells [16]. However, if they are to be used in biocomposites with an inorganic matrix, WNs need to undergo some kind of pretreatment. These processes can be divided into two basic types: physical and chemical methods, where physical pretreatment processes are usually of mechanical nature [17]. Physical methods of pretreatment predominantly have the goal of changing the shape or size of the lignocellulosic materials; the most commonly used mechanical process is grinding. Physical methods can also influence the chemical composition, causing the removal of pectin, hemicellulose and lignin [18–20]. However, chemical pretreatment is an inevitable step in creating lignocellulosic biocomposites due to the hydrophilic nature of the LCM caused by the high number of hydroxyl groups enveloping the surface [21], organic groups present on the surface of the lignocellulose, as well as pectin, waxes and sugars, which may impede the setting of the biocomposite matrix. Without compatibilization, poor adhesion between the matrix and the filler occurs, and no interphase is created, leading to poor mechanical properties of the composite. Various types of chemical pretreatments are used that differ in the type of chemical applied, such as acids, bases (mercerization), ionic liquids, oxidizing agents or organosols [22,23].

One of the promising inorganic matrixes for WN composites are geopolymers. Geopolymers are aluminosilicate materials obtained by the alkaline or acid activation of aluminosilicate powder precursors. These kinds of novel materials are a plausible ecologically acceptable and sustainable replacement for Portland cement, which is occasionally used as an inorganic matrix in composite materials. The manufacture of geopolymers involves the use of low-cost waste materials like fly ash or metakaolin, lower energy consumption and lower CO₂ emissions [24]. Activation solutions of alkaline-activated geopolymers are usually solutions of potassium or sodium hydroxide, solutions of sodium or potassium soluble silicates, better known as water glass, or their combinations [25]. According to the literature, agro-industrial waste material ashes are used as raw materials for geopolymer concrete [26] or geopolymers are reinforced with various natural fibers (sisal, jute, cotton stalk) to enhance their mechanical properties [27]. However, to our knowledge, no biocomposites of geopolymer matrix and waste nutshell have so far been studied for use in civil engineering. Considering the sustainability, low cost and low carbon footprint

of such biocomposites, geopolymers were chosen as the model inorganic matrix for WN biocomposites in this study.

This work is an extensive investigation of the influence of alkaline treatment, employing the traditional NaOH solution and Ca(OH)₂ suspension, on waste almond and hazelnut nutshells. The composition and the properties of the WNs were characterized after the different pretreatment regimes using X-ray diffraction analysis (XRD) to determine the change in the crystallinity index. Fourier-transform infrared (FTIR) spectroscopy in combination with simultaneous differential thermal and thermogravimetric analysis (DTA/TGA) was employed to determine the change in the composition of the WN, while scanning electron microscopy (SEM) was used to determine the change in the morphology of the almond and hazelnut nutshells, as well as to investigate the precipitation of Na and Ca compounds on the surface of the WN. Furthermore, water and diiodomethane contact angles were determined, and free-surface energies were calculated for all the WN and chosen model geopolymer matrix samples. Adhesion parameters were then calculated to determine which combination of pretreatment and geopolymer type could result in an optimal inorganic biocomposite and to carve the path to future studies involving the most promising biocomposite candidates.

2. Materials and Methods

2.1. Materials

Waste almond nutshell (AN) and waste hazelnut nutshell (HN) were donated by small farmers from the Šibenik-Knin and Zagreb County, Croatia. NaOH solutions were prepared by dissolving NaOH microgranules (p.a., Gram-mol, Zagreb, Croatia) in demineralized water, while milk of lime was prepared by mixing freshly prepared CaO (obtained by calcination of CaCO₃, p.a., Merck, Darmstadt, Germany) and demineralized water in a 1:7 ratio. Geopolymers were prepared from fly ash acquired from the Plomin power station (Plomin, Croatia) and metakaolin, i.e., calcined commercial kaolin clay (technical grade, VWR Chemicals, Paris, France) activated by sodium (technical grade, VWR Chemicals, Paris, France) or potassium (technical grade, Ivero, Zagreb, Croatia) water glass combined with 12 M solution of NaOH or KOH (p.a., Gram-mol, Zagreb, Croatia).

2.2. Sample Preparation

Waste nutshells were milled using a manual grinder, after which they were treated with alkaline solutions (Figure 1). NaOH treatment was carried out using 3, 6 and 9% solutions for 1 and 2.5 h at 80 °C, while milk of lime was prepared using a 1:7 ratio of CaO and demineralized water. Treatment with milk of lime was accomplished by mixing WN and milk of lime in a 1:8 ratio and processed at 80 °C for 1 and 2.5 h, while another batch of treated WN was prepared at room temperature for 24 h.

In Table 1, the mass fractions of the particle size distribution for both waste nutshells after grinding are given.

Table 1. Mass fractions of the particle size distribution for hand-sieved waste nutshells.

Fraction (mm)	>2.5	2.5–1.25	1.25–0.8	<0.8
Hazelnut WN (wt%)	4.35	69.90	11.18	13.77
Almond WN (wt%)	6.7	68.21	12.05	12.18

Geopolymer samples were prepared by activating metakaolin or fly ash with a 12 M NaOH or KOH solution mixed with sodium or potassium water glass to achieve a water-to-solid ratio of 0.66 and a molar ratio Al:Na,K = 1:1. Geopolymer pastes were poured into molds after 5 min of mixing and cured at room temperature or 40 °C. The geopolymer samples prepared using metakaolin were denoted as M and those using fly ash as FA, while sodium activation solutions were named Na, and potassium activation solutions were named K. Geopolymers cured at room temperature were denoted as RT and the curing at

40 °C was denoted as 40C. Figure 2 shows five different geopolymer plate samples that were used for measuring the contact angles.



Figure 1. Waste almond and hazelnut nutshells: (a) as received waste nutshells, (b) ground waste nutshells, or (c) nutshells treated with milk of lime for 2.5 h at 80 °C.

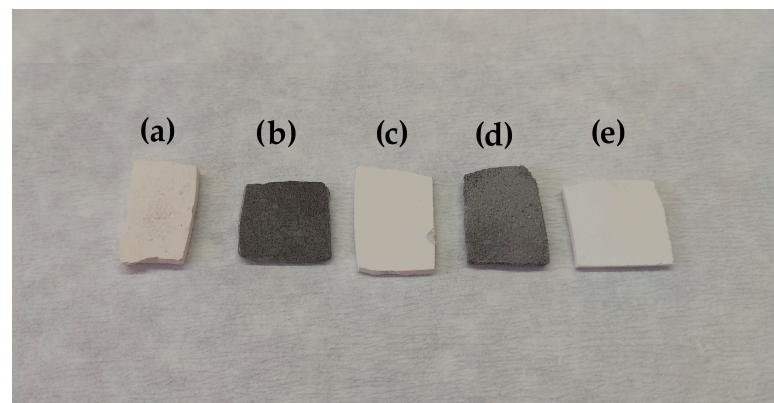


Figure 2. Five different geopolymer samples: (a) MNaRT; (b) FANaRT; (c) MKRT; (d) FAKRT; (e) MNa40C.

For most analyses, the shape and the form of the treated ground WN were not suitable; thus, WNs were further milled in an electric mill to produce fine powders, which were then pressed into small tablets of 13 mm diameter and used in further analyses.

2.3. Characterization

The crystallinity index (*CI*) was determined from the diffraction patterns acquired by XRD analysis on a Shimadzu XRD 6000 instrument (Shimadzu, Tokyo, Japan) with CuK α radiation in the 2 θ range from 5 to 40° with a 2 θ step of 0.02° and 0.6 s counting time. The Fityk program (version 1.3.1) [28] was used for data processing, and nonlinear curve fitting used the Pseudo-Voigt function in order to calculate the crystallinity indices. Crystallinity indices were calculated using Equation (1), where $A_{\text{Crystalline}}$ was obtained by fitting the crystalline contribution (peaks at 15.25°, 18.52°, 21.84° and 34.8°) and A_{Model} was obtained by adding the amorphous contribution (broad hump centered at 22°) to the modelled data of the crystalline peaks.

$$CI = \frac{A_{\text{Crystalline}}}{A_{\text{Model}}} \quad (1)$$

The efficiency of the removal of specific undesirable components and groups from the waste nutshells was determined using FTIR analysis, which was carried out using a Bruker Vertex 70 spectrometer (Bruker Optics, Karlsruhe, Germany) in attenuated total reflectance mode (ATR) on samples pressed on a diamond, and the spectra measured between 400 and 4000 cm^{-1} , with a spectral resolution of 2 cm^{-1} and an average of 32 scans. FTIR analysis results were complemented by results of simultaneous DTA/TGA analyses using the Netzsch STA 409 analyzer (Netzsch-Gerätebau GmbH, Selb, Germany) with a heating rate of 10 $^{\circ}\text{C min}^{-1}$ from room temperature to 1000 $^{\circ}\text{C}$. A Tescan Vega 3 scanning electron microscope (Tescan, Brno, Czech Republic) operating at 10 kV was used for observing the changes in the morphology of the WN samples before and after the pretreatments. Samples were fixed on specimen holders with double-sided carbon conductive tape and gold-coated using a Quorum SC 7620 sputter coater (Quorum Technologies, Loughton, United Kingdom). The contact angle was determined by the sessile-drop method using the goniometer DataPhysics OCA 20 Instrument (DataPhysics Instruments GmbH, Filderstadt, Germany) which projects the image of the drop onto the computer screen via the video system and determines the position of the drop with an accuracy of ± 1 mm. The surface free energy (SFE) of all the samples, γ , as well as polar (γ^p) and disperse (γ^d) components of the SFE were calculated using the Owens–Wendt model, using the contact angle values of three different drops of the two testing liquids, water and diiodomethane. The adhesion parameters of binary systems comprised of nutshell and the geopolymer were calculated using the following equations:

Interfacial free energy (γ_{12})—OWRK model:

$$\gamma_{12} = \gamma_1 + \gamma_2 - 2\sqrt{\gamma_1^d \gamma_2^d} - 2\sqrt{\gamma_1^p \gamma_2^p} \quad (2)$$

Work of adhesion (W_{12}):

$$W_{12} = \gamma_1 + \gamma_2 - \gamma_{12} \quad (3)$$

Spreading coefficient (S_{12}):

$$S_{12} = \gamma_1 - \gamma_2 - \gamma_{12} \quad (4)$$

where γ_1 is the surface free energy of the geopolymer and γ_2 the surface free energy of the nutshell [29].

3. Results and Discussion

3.1. Crystallinity Index

The XRD patterns of the untreated AN and HN samples as well as of AN and HN samples pretreated with 9% NaOH for 2.5 h at 80 $^{\circ}\text{C}$ and milk of lime for 24 h at room temperature are shown in Figure 3. All the patterns appear similar, with a sharp peak around 22 $^{\circ}$ 2 θ and two weaker peaks around 15 and 17 $^{\circ}$ 2 θ , while a small and wide peak can be observed at 35 $^{\circ}$ 2 θ . These peaks represent the crystalline part of the cellulose molecule and confirm that the nature of the cellulose in the WN is cellulose I (ICDD 00-056-1718) [30]. No significant shift in the peak position after the pretreatment can be observed, which indicates that the cellulose remains in the cellulose I form. Low concentrations of alkaline solutions do not appear to induce a change from cellulose I to cellulose II, as reported by Chen et al. [30] for bamboo fibers treated with 6, 8 and 10% NaOH solutions and Sun et al. [31] regarding poplar treated by a low concentration $\text{Ca}(\text{OH})_2$ solution. Only one new peak at 29 $^{\circ}$ 2 θ (Figure 3c,f) appears after the pretreatment with milk of lime, which is the result of $\text{Ca}(\text{OH})_2$ deposition on the surface of the WN, which transforms into calcite over time [32,33]. The presence of calcite after milk-of-lime treatment was also reported by Ferreira et al. [32] for bamboo, as well as by Sanchez-Echeverri et al. [33] for sisal fibers.

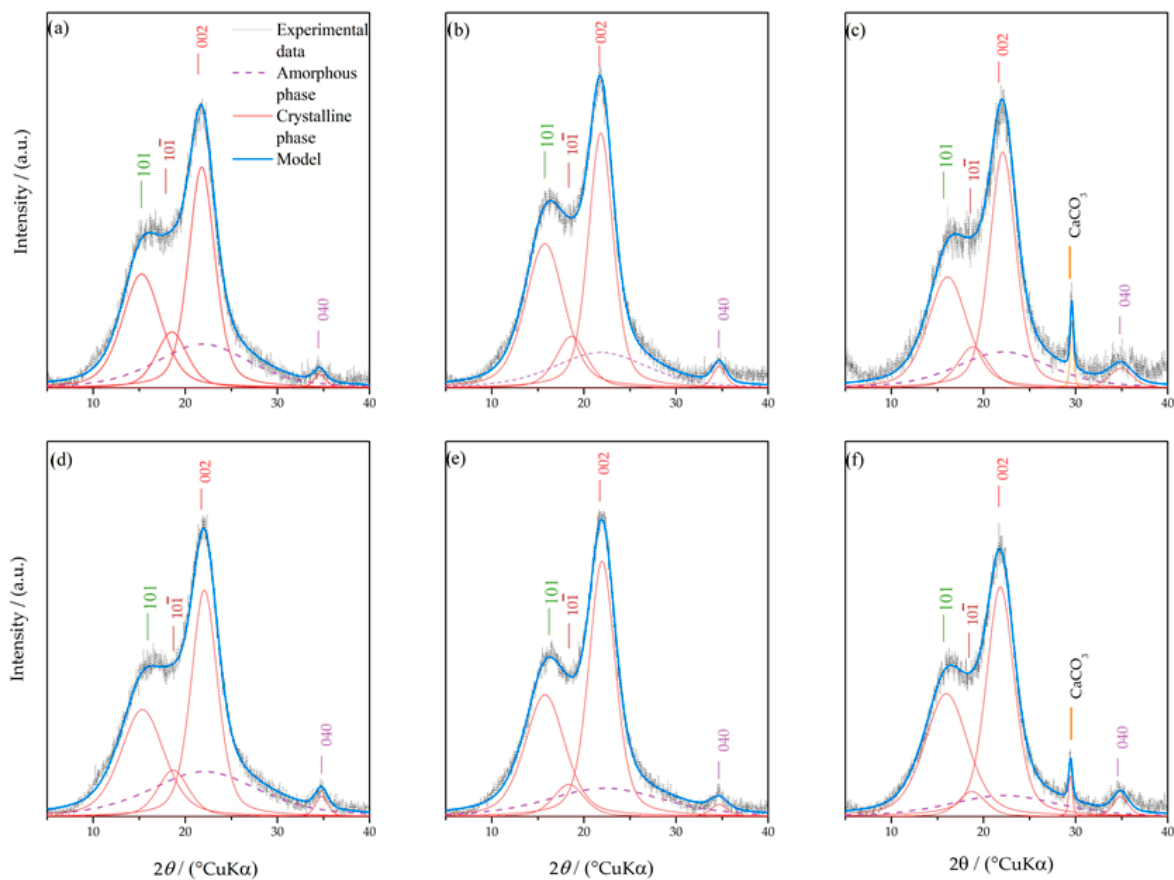


Figure 3. XRD results of (a) untreated HN, (b) HN treated with 6% NaOH for 1 h at 80 °C, (c) HN treated with milk of lime for 24 h at RT, (d) untreated AN, (e) AN treated with 6% NaOH for 1 h at 80 °C, and (f) AN treated with milk of lime for 24 h at RT.

The crystallinity indices calculated by fitting the crystalline and amorphous contribution to the experimental data using the Fityk software are shown in Table 2. As can be seen, the crystallinity of the AN and HN increases with the increase in NaOH concentration and the duration of treatment. The CI increase in WN with the alkaline pretreatment is the consequence of the rearrangement of the cellulosic chains as well as the removal of amorphous and undesired components of WN, such as hemicellulose, amorphous cellulose, pectin, lignin, etc.; similar results were reported by other researchers [33,34].

Table 2. Crystalline indices of the untreated and pretreated waste nutshells.

	Untreated		Ca(OH) ₂				NaOH				
Concentration (%)	-	-	12.5	25	3	6	9	-	-	-	
Temperature (°C)	-	-	80	25	-	80	-	-	-	-	
Duration (h)	-	-	1	2.5	24	1	2.5	1	2.5	1	2.5
Hazelnut CI (%)	55	66	71	66	60	67	63	65	77	61	
Almond CI (%)	51	63	68	66	63	61	65	63	65	68	

3.2. FTIR Analysis

Figure 4 shows the FTIR spectra for the almond and hazelnut nutshells. Both spectra show highly similar features; therefore, they will be characterized conjointly. The spectra show distinct lignocellulosic bands for untreated WN, and changes in those bands with the alkaline pretreatment. The results are comparable to other research regarding the alkaline treatment of natural fibers, such as those by Ferreira [32], Sanchez-Echeverri [33],

Rahman [35] and Barreto [36]. All samples show a reduction in their band intensities, especially for the bands present around 3200 cm^{-1} , which are the result of the $-\text{OH}$ groups present in the LCM and water. These are also bridging groups between hemicellulose, cellulose and lignin that are present on the surface of the LCM, which restrict the adhesion between the WN and the inorganic binder in biocomposites [30]. The CH stretching vibrations, present in the spectra at 2900 cm^{-1} as bands next to the OH stretching vibrations, represent aliphatic constituents in cellulose and hemicellulose. Diminishing intensities in these bands demonstrate the removal of undesired surface OH groups and hemicellulose from the waste nutshell [32,33]. Another good indication of the removal of undesired constituents is the reduction and sharpening of the band intensities in the region between 1750 and 800 cm^{-1} . Bands centered around 1730 cm^{-1} arise due to the carbonyl group ($\text{C}=\text{O}$), which is present in hemicellulose and different extractives, while the groups of bands from 1500 to 1650 cm^{-1} are the result of aromatic skeletal and ring vibrations in lignin and extractives [32,36,37].

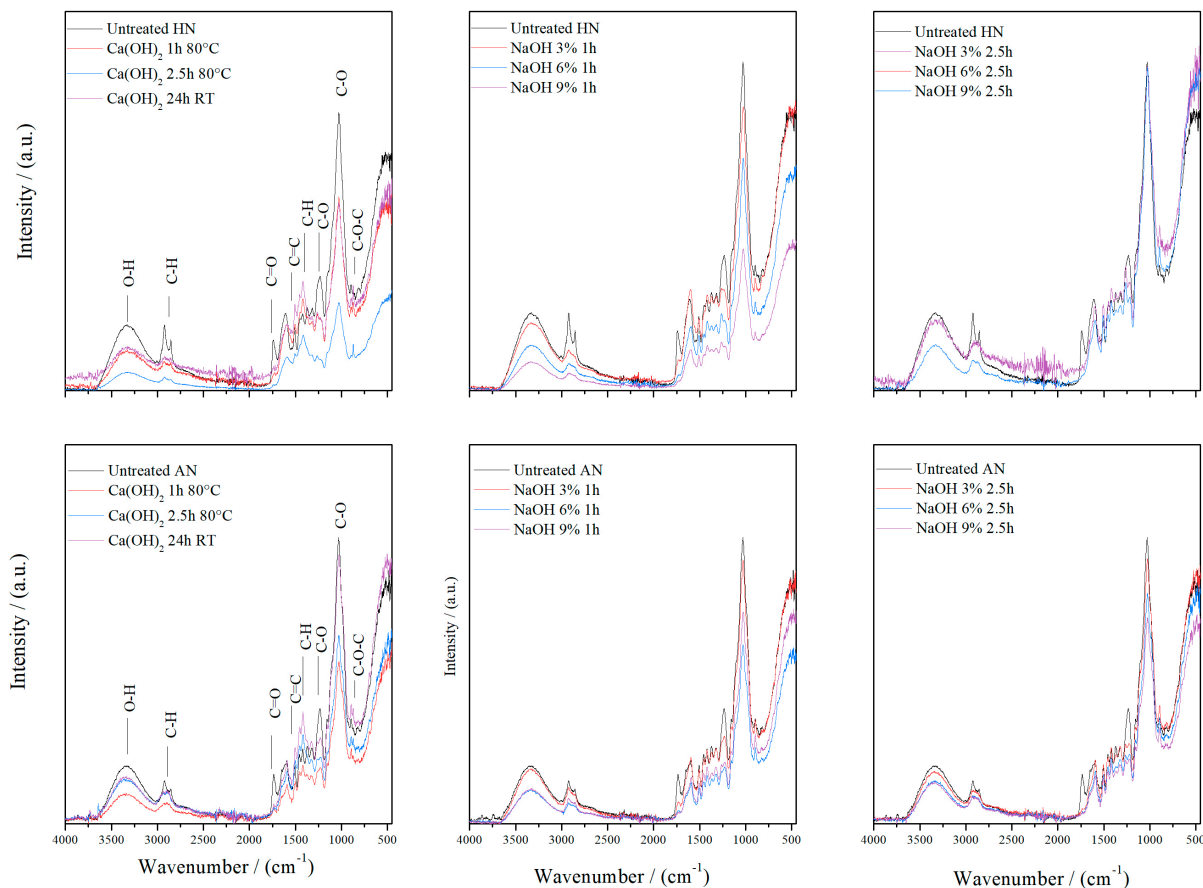


Figure 4. FTIR spectra of untreated and treated waste hazelnut and almond nutshells.

Bands arising in the range from 1350 to 1500 cm^{-1} belong to carbonyl-group stretching in lignin and O-H in-plane bending and C-H bending in lignin, hemicellulose and cellulose. These peaks decrease with the pretreatment, although for the samples treated with milk of lime, the loss of intensities is modest in comparison with those treated with NaOH, which could indicate an inadequate removal of undesired constituents with the milk of lime. Stretching of the C-O bonds in the polysaccharides present in the LCM and O-H in-plane bending is manifested as a sharp peak at 1232 cm^{-1} that loses its intensity with the pretreatment. The highest intensity peak at 1029 cm^{-1} corresponds to C-O stretching vibrations in the cellulose, with no significant loss in intensity. Two close peaks at 896 and 873 cm^{-1} correspond to C1-H deformation in the cellulose molecules and precipitated CaCO_3 , respectively [33,37,38]. The latter can only be found in the samples treated with

the milk of lime, which is in concordance with the XRD results and the Sanchez-Echeverri et al. report [33].

3.3. Simultaneous DTA/TGA Analysis

Thermal stability of the lignocellulosic materials can indicate the effectiveness of the pretreatment and the removal of undesired constituents. Commonly, DTA/TGA analysis of LCM consists of a convoluted exothermal effect, with a leading effect that appears as a shoulder or a visible separate peak in the thermograms at 200–350 °C that correlates to the burning of the hemicellulose and lignin, and a following effect, which is a direct consequence of the cellulose burning in the range from 350 to 500 °C [39]. Consequently, the absence or mitigation of the hemicellulose and lignin burning effect shows the scope of removal of these already mentioned components. The thermograms displayed in Figure 5 for HN and Figure 6 for AN were chosen as representative among all the analyzed samples to exemplify the changes that occur with the pretreatment. Figure 5 shows that the pretreatment of the HN is effective due to the absence of the first thermal effect in the samples treated with NaOH, while the WN treated with milk of lime still has the shoulder at 350 °C present, which, in combination with the FTIR spectra in Figure 4, confirms that the milk-of-lime pretreatment does not thoroughly remove hemicellulose and lignin from the waste nutshell.

Similar curves can be observed in Figure 6. Thermograms of waste almond nutshell corroborate the conclusion derived from the FTIR analysis of AN as well as the DTA/TGA analysis of HN, i.e., that the milk-of-lime treatment does not effectively remove hemicellulose and lignin from AN.

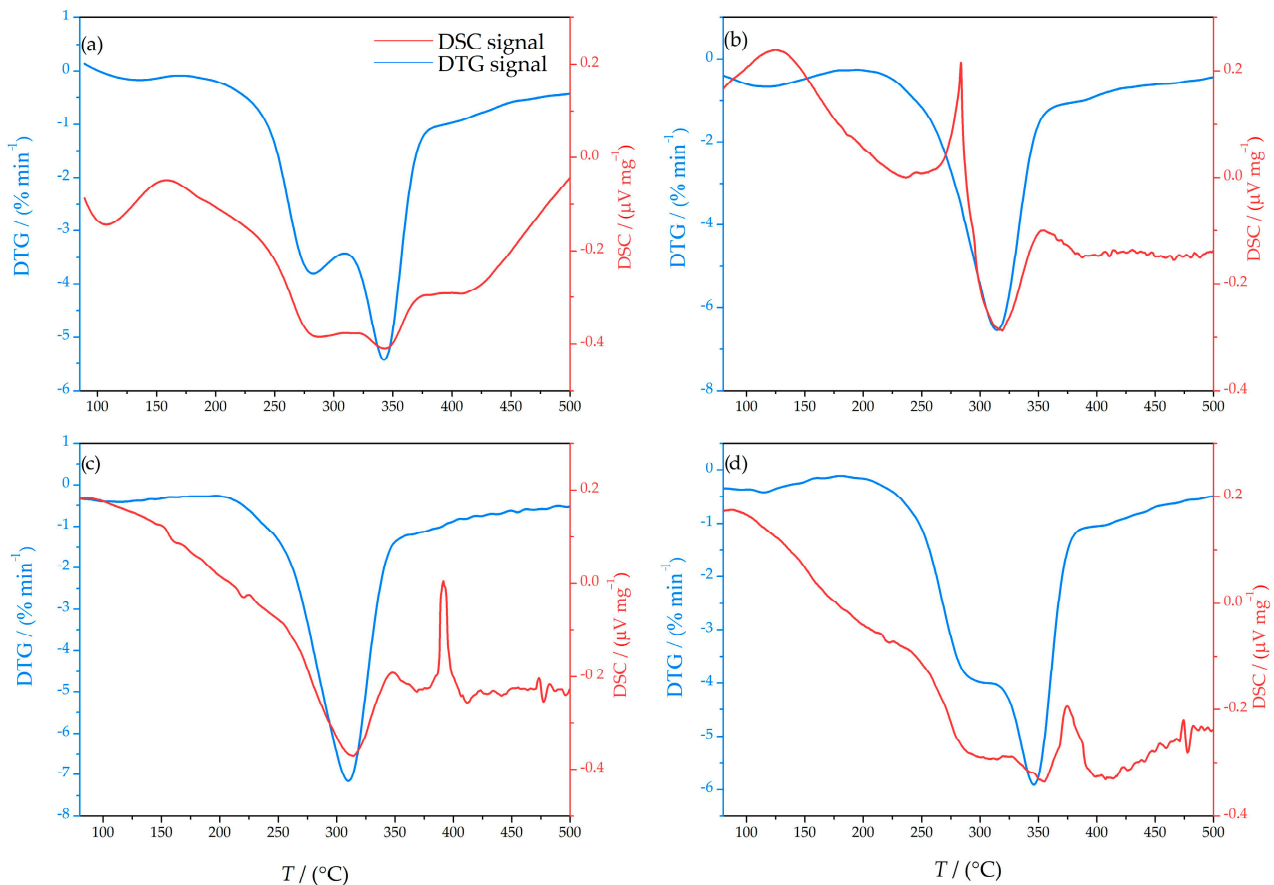


Figure 5. Simultaneous DTA/TGA analysis results for (a) untreated HN, (b) HN treated with 9% NaOH for 1 h at 80 °C, (c) HN treated with 9% NaOH for 2.5 h at 80 °C, and (d) HN treated with milk of lime for 1 h at 80 °C.

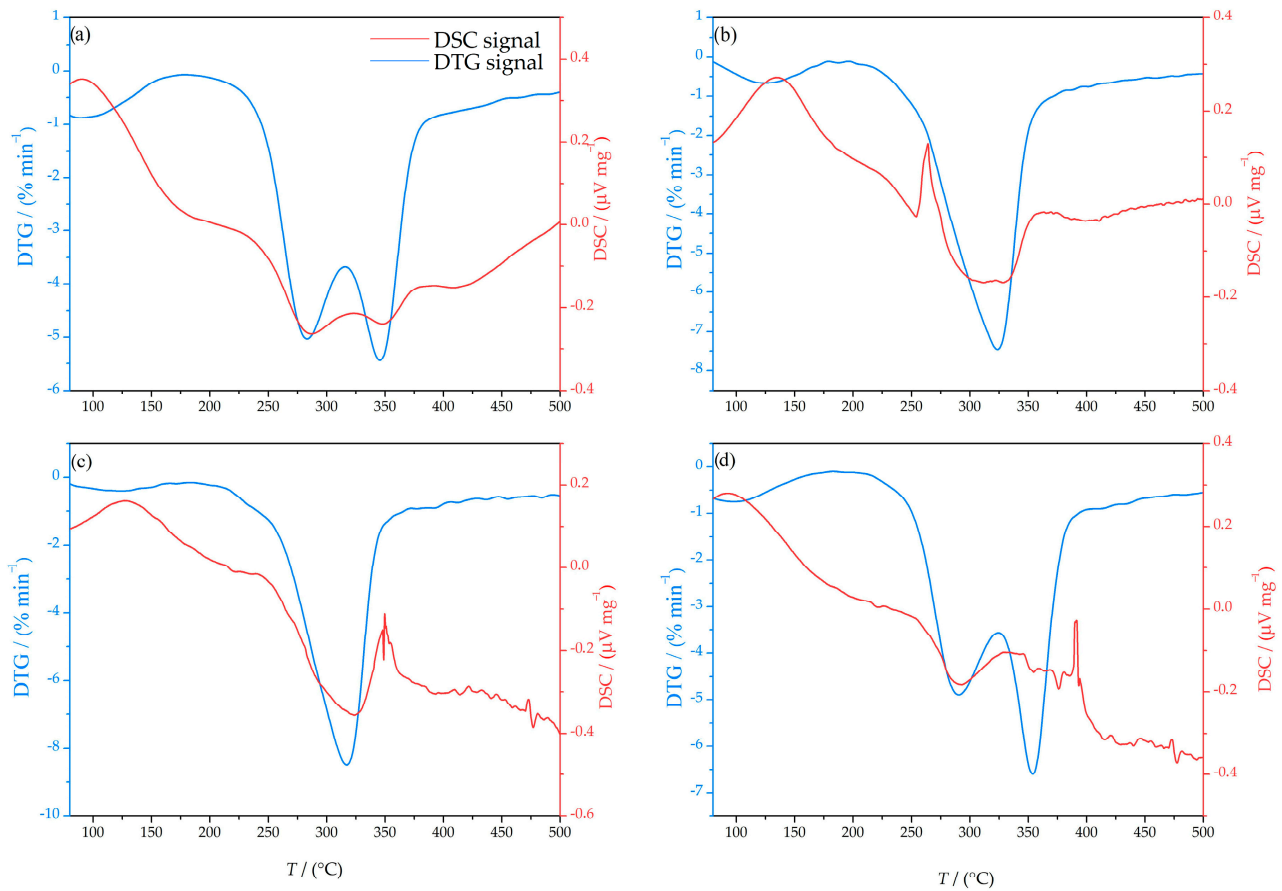


Figure 6. Simultaneous DTA/TGA analysis results for (a) untreated AN, (b) AN treated with 9% NaOH for 1 h at 80 °C, (c) AN treated with 9% NaOH for 2.5 h at 80 °C, and (d) AN treated with milk of lime for 1 h at 80 °C.

3.4. SEM Analysis

Figures 7 and 8 show micrographs of waste hazelnut and almond nutshells treated with NaOH. The porous and cell-like structure of the almond nutshell could indicate good insulating properties of its biocomposites. It can be observed that with the change in the pretreatment conditions, the roughness of the WN surface is increased. Furthermore, the nature of the precipitate deposited on the surface of the WN changes: with the increase in the concentration and time of pretreatment, the appearance changes from separate crystalline particles to films. These precipitates could facilitate the linking between WN and the inorganic matrix as interlocking spots, as well as act as seeds for the formation of new phases during the curing of the binder.

Figure 9 shows micrographs of waste hazelnut and almond nutshells treated with milk of lime. Milk-of-lime pretreatment displays similar results to the NaOH treatment, but the precipitation of CaCO_3 is immense, while the appearance of the precipitate changes with the conditions as well. The change from smaller particulates to a mixture of particulates and film deposits can clearly be observed in Figure 9. Moreover, the difference in the shape of the precipitate can be seen, depending on the type of nutshell. While the AN precipitate from the pretreatment at 80 °C has a regular cauliflower-like structure, that of the HN shows smaller elongated particles. Both WNs possess thin needle-like particles when treated at room temperature for 24 h.

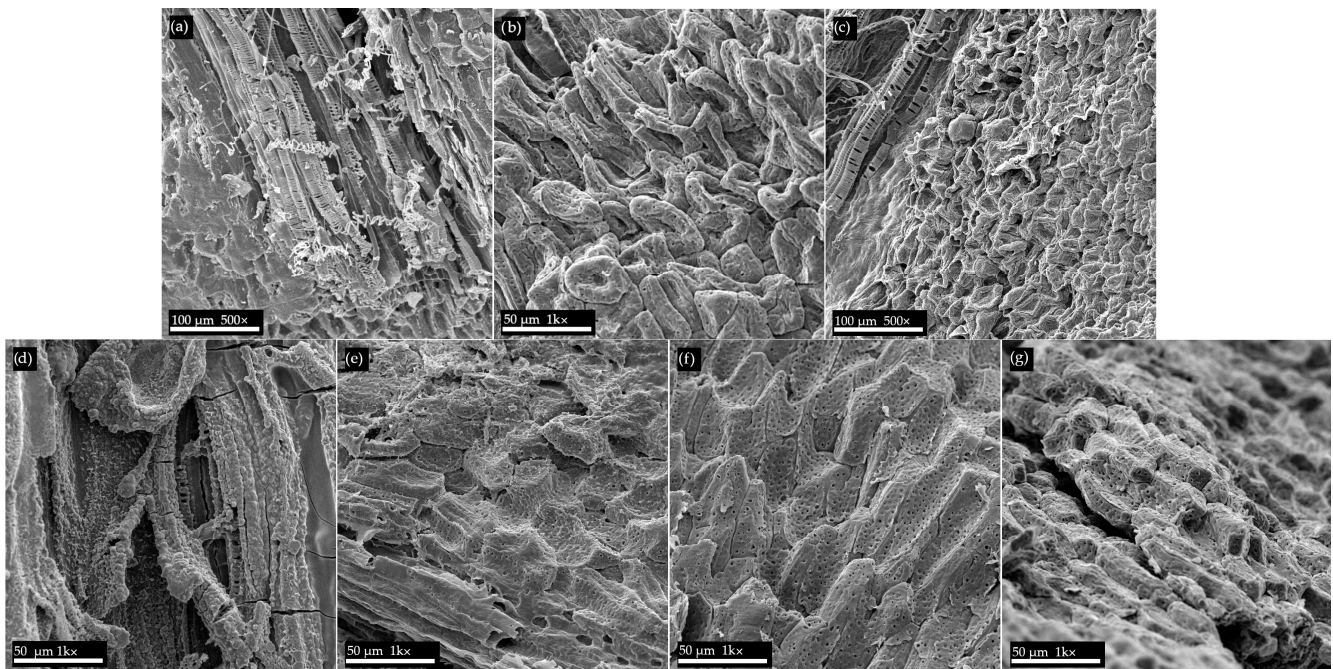


Figure 7. Micrographs of waste hazelnut nutshell: (a) untreated; (b) treated with 3% NaOH for 1 h at 80 °C; (c) treated with 6% NaOH for 1 h at 80 °C; (d) treated with 9% NaOH for 1 h at 80 °C; (e) treated with 3% NaOH for 2.5 h at 80 °C; (f) treated with 6% NaOH for 2.5 h at 80 °C; (g) treated with 9% NaOH for 2.5 h at 80 °C. All the micrographs were acquired using a 10 kV beam intensity.

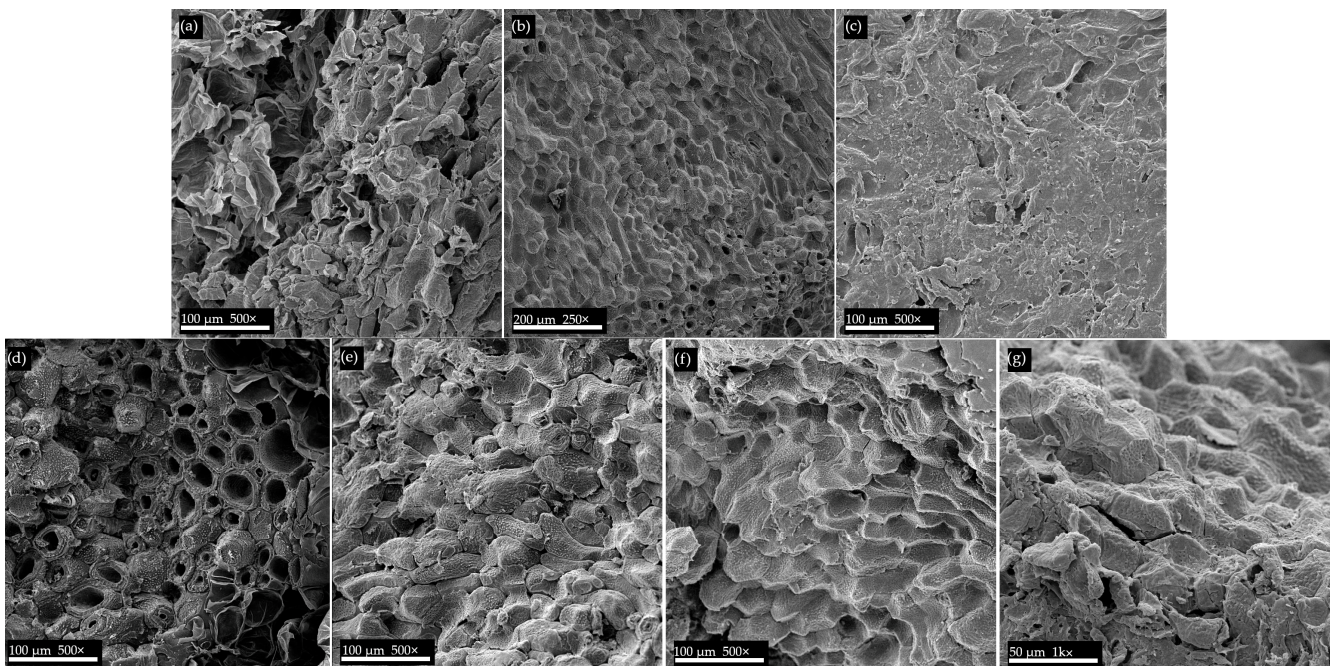


Figure 8. Micrographs of waste almond nutshell: (a) untreated; (b) treated with 3% NaOH for 1 h at 80 °C; (c) treated with 6% NaOH for 1 h at 80 °C; (d) treated with 9% NaOH for 1 h at 80 °C; (e) treated with 3% NaOH for 2.5 h at 80 °C; (f) treated with 6% NaOH for 2.5 h at 80 °C; (g) treated with 9% NaOH for 2.5 h at 80 °C. All the micrographs were acquired using a 10 kV beam intensity.

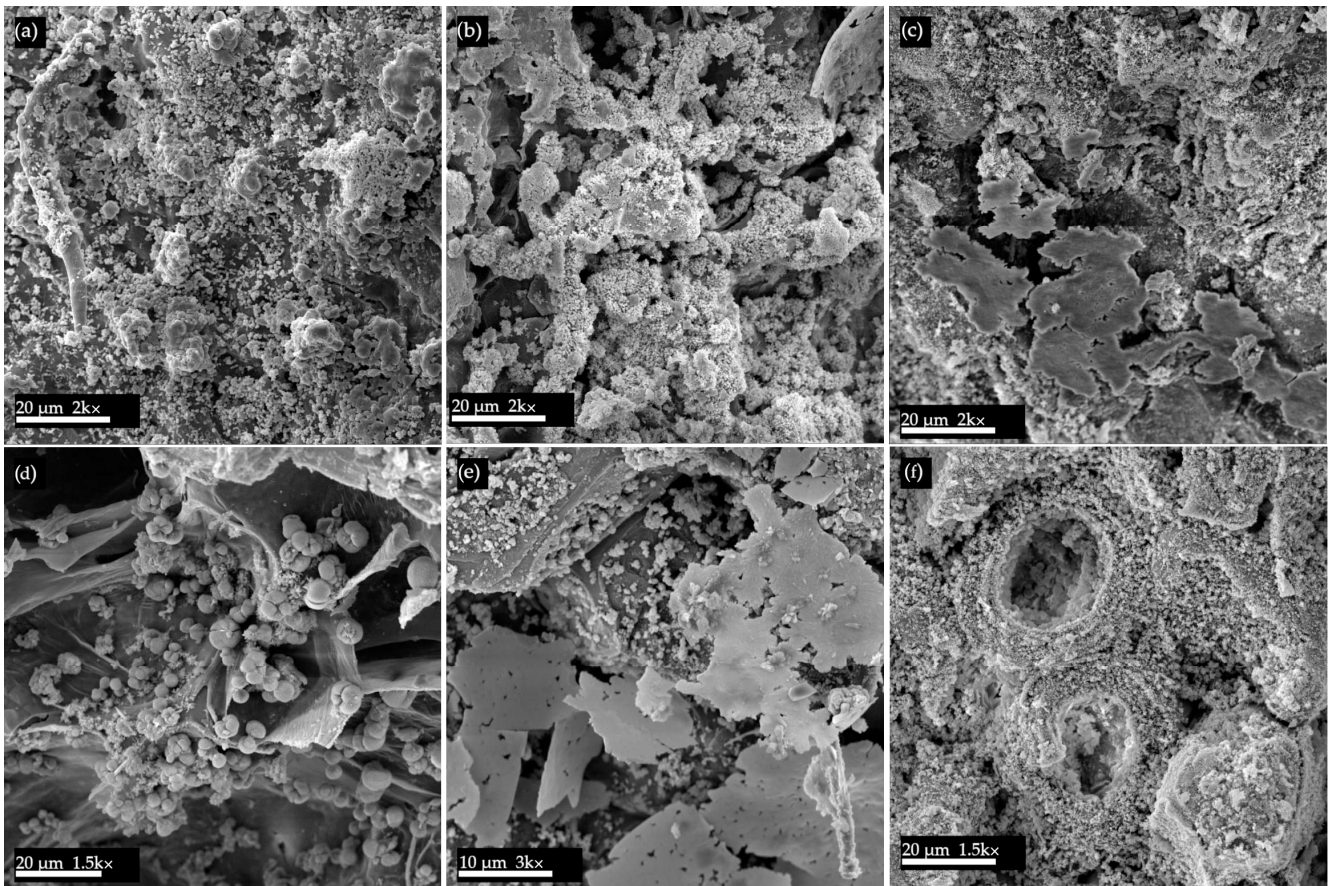


Figure 9. Micrographs of waste nutshell treated with milk of lime: (a) HN treated for 1 h at 80 °C; (b) HN treated for 2.5 h at 80 °C; (c) HN treated at RT for 24 h; (d) AN treated for 1 h at 80 °C; (e) AN treated for 2.5 h at 80 °C; (f) AN treated at RT for 24 h.

3.5. Surface Free Energy and Adhesion Parameters

Surface free energies (SFEs) for both WNs have been calculated and are shown in Table 3. The calculated values (γ) for HN show no significant trend with the change in the pretreatment conditions, while those for the treated AN are slightly smaller in comparison with the untreated AN. However, the polar component (γ_p) exhibits a sharp reduction with the $\text{Ca}(\text{OH})_2$ pretreatment for HN and with all types of pretreatments for AN, which could indicate the desired depletion from the surface of the WN of different extractive components and hydroxyl groups, which are hydrophilic and increase the polar component of the SFE. This is in agreement with the FTIR results. Judging from the SEM micrographs, the rise in the SFE values is the direct consequence of the change in the morphology of the surface as well as the deposition of the Na and Ca crystalline phases.

In Table 4, the SFE values for the different geopolymers samples are shown. Geopolymers were chosen as a model inorganic matrix as they represent new and promising mineral binders for use in the construction industry and in civil engineering. The geopolymer samples were chosen to elucidate the influence of the type of solid precursors (M—metakaolin; FA—fly ash), activation solution (Na—sodium activators; K—potassium activators) and different curing conditions (RT—room temperature; 40–40 °C) on the surface properties of the geopolymers and, consequently, the adhesion between geopolymers and waste nutshells. While samples obtained from metakaolin have similar values for the disperse and polar components of the surface free energy, the fly-ash samples have a much larger contribution of the polar component to the total SFE.

Table 3. SFE values for waste nutshells.

OWRK		$\gamma^d, \text{mJ m}^{-2}$		$\gamma^p, \text{mJ m}^{-2}$		$\gamma, \text{mJ m}^{-2}$		
		Hazelnut	Almond	Hazelnut	Almond	Hazelnut	Almond	
Untreated nutshell		25.0	36.7	5.2	13.8	30.2	50.5	
Ca(OH) ₂	1 h, 80 °C	30.1	29.8	0.3	2.1	30.4	31.9	
	2.5 h, 80 °C	33.5	39.9	0.1	3.4	33.6	43.3	
	24 h, RT	32.6	38.7	0.4	1.6	33	40.3	
NaOH	3%	1 h, 80 °C	23.5	36.4	4.8	1.8	28.3	38.2
		2.5 h, 80 °C	25.8	35.9	6.0	3.4	31.8	39.3
	6%	1 h, 80 °C	18.0	29.1	6.5	3.9	24.5	33.0
		2.5 h, 80 °C	30.7	38.4	9.2	4.6	39.9	43.0
	9%	1 h, 80 °C	13.4	22.4	7.3	6.6	20.7	29.0
		2.5 h, 80 °C	32.3	34.4	8.8	1.7	41.1	36.1

Table 4. Surface free energies of different geopolymer samples.

Geopolymer Sample	OWRK		
	$\gamma_1^d, \text{mJ m}^{-2}$	$\gamma_1^p, \text{mJ m}^{-2}$	$\gamma_1, \text{mJ m}^{-2}$
MNa40C	38.0	24.4	62.4
MNaRT	36.2	31.5	67.7
MKRT	38.5	37.7	76.2
FANaRT	11.2	63.7	74.9
FAKRT	20.3	52.6	72.9

In Tables 5 and 6, values of the interfacial free energy (γ_{12}), work of adhesion (W_{12}) and spreading coefficient (S_{12}) for all the samples calculated by the OWRK model are given. The conditions for achieving optimal adhesion between two components are a maximal thermodynamic work of adhesion ($W_{12} = \text{max}$), a positive value of the spreading coefficient ($S_{12} \geq 0$) and a minimal value of interfacial free energy ($\gamma_{12} = \text{min}$) [29].

Table 5. Interfacial free energy (γ_{12}), work of adhesion (W_{12}) and spreading coefficient (S_{12}) values for the hazelnut nutshell and geopolymers.

Hazelnut Nutshell	MNa40C			MNaRT			MKRT			FANaRT			FAKRT				
	γ_{12}	W_{12}	S_{12}	γ_{12}	W_{12}	S_{12}	γ_{12}	W_{12}	S_{12}	γ_{12}	W_{12}	S_{12}	γ_{12}	W_{12}	S_{12}		
Untreated nutshell	8.4	84.2	28.4	12.1	85.7	25.3	16.3	90.0	27.0	34.4	70.7	10.3	24.9	78.1	17.7		
Ca(OH) ₂	1 h, 80 °C	16.7	73.1	12.4	25.8	72.2	11.5	31.6	75.0	14.2	58.6	56.7	−14.1	45.7	57.5	−3.3	
	2.5 h, 80 °C	21.4	74.7	7.5	27.9	73.3	6.1	33.9	76.0	8.7	63.3	45.2	−22.0	49.5	56.9	−10.2	
	24 h, RT	19.0	76.5	10.5	25.1	75.5	9.5	30.8	78.4	12.4	58.8	49.1	−16.9	45.6	60.3	−5.7	
NaOH	3%	1 h, 80 °C	9.3	81.4	24.9	13.1	82.8	26.3	17.4	87.0	30.5	35.0	68.2	11.6	25.7	75.4	18.8
		2.5 h, 80 °C	7.3	87.0	23.2	10.8	88.7	25.0	14.8	93.2	29.5	32.7	74.1	10.3	23.3	81.4	17.7
	6%	1 h, 80 °C	9.4	77.5	28.5	12.5	79.6	30.6	16.8	83.9	34.9	29.7	69.7	20.7	22.2	75.1	26.1
		2.5 h, 80 °C	4.0	98.3	18.5	6.9	100.7	20.9	10.0	106.0	26.2	28.4	86.4	6.6	18.8	93.9	14.1
	9%	1 h, 80 °C	11.3	71.8	30.5	14.0	74.3	33.0	18.3	78.6	37.2	27.4	68.2	26.8	21.4	72.1	30.8
		2.5 h, 80 °C	4.1	99.4	17.2	7.0	101.7	19.5	10.3	107.0	24.8	29.7	86.4	4.2	19.7	94.2	12.0

Table 6. Interfacial free energy (γ_{12}), work of adhesion (W_{12}) and spreading coefficient (S_{12}) values for the almond nutshell and geopolymers.

Almond Nutshell		MNa40C			MNaRT			MKRT			FANaRT			FAKRT			
		γ_{12}	W_{12}	S_{12}													
Untreated nutshell		1.5	111.4	10.5	3.6	114.5	13.6	5.9	120.8	19.8	24.6	100.8	−0.2	14.9	108.4	7.5	
Ca(OH) ₂	1 h, 80 °C	12.7	81.7	17.9	17.6	81.9	18.1	22.5	85.5	21.8	46.1	60.7	−3.1	34.5	70.1	6.4	
	2.5 h, 80 °C	9.5	96.2	9.6	14.1	96.8	10.4	18.3	101.2	14.5	45.1	73.0	−13.6	32.3	83.8	−2.8	
	24 h, RT	13.4	89.3	8.8	18.8	89.2	8.6	23.6	92.2	12.3	52.0	63.2	−17.4	38.6	74.6	−6.0	
NaOH	3%	1 h, 80 °C	13.0	87.7	11.5	18.3	87.6	11.1	23.0	91.4	14.9	50.2	62.9	−13.5	37.2	73.8	−2.6
		2.5 h, 80 °C	9.6	92.2	13.5	14.1	92.9	14.1	18.4	97.4	18.4	43.5	70.8	−7.9	31.3	80.8	2.1
	6%	1 h, 80 °C	9.3	86.1	20.1	13.5	87.2	21.1	17.9	91.3	25.3	39.1	68.8	2.8	28.4	77.4	11.4
		2.5 h, 80 °C	7.8	97.7	11.7	12.0	98.6	12.7	15.8	103.1	17.4	40.9	77.0	−9.0	28.8	87.0	1.09
	9%	1 h, 80 °C	7.7	83.7	25.8	10.9	85.7	27.8	14.9	90.2	32.3	30.4	73.4	15.6	21.9	79.9	22.0
		2.5 h, 80 °C	13.3	85.1	13.0	18.6	85.1	13.0	23.5	88.7	16.6	49.9	61.1	−11.0	37.2	71.7	−0.5

When taking into account the criteria of optimal adhesion, the treatment of nutshells with 6% NaOH at 80 °C for 2.5 h seems to be the best in the case of hazelnut for all the studied geopolymers and should result in a biocomposite with optimal properties. This is in concordance with the overall characterization results, which show the best removal of unwanted extractives, lignin and hemicellulose for these pretreatment conditions. For almond nutshell, the results are quite contradictory. It would seem at first that the best adhesion properties are achieved by using the untreated nutshell. However, literature references [16] as well as the nutshell characterization results presented in this work indicate that this is not the case, because the surface of the nutshell is full of undesired components which prevent good bonding between the geopolymer and the nutshell and impede the setting of inorganic binders. Therefore, according to the adhesion parameters, the second-best option would again be the treatment with 6% NaOH for 2.5 h at 80 °C, except in the case of the geopolymer obtained from sodium-activated fly ash cured at RT, where treatment of almond nutshell with 9% NaOH for 1 h at 80 °C seems to be the best choice. It is important to note that these results are only indicative, and it is necessary to carry out the preparation of biocomposites and their characterization to confirm the results. However, this work gives a detailed account of the influence of a particular type of nutshell treatment on its properties and serves as a guideline for further tests of geopolymer—waste nutshell biocomposites.

4. Conclusions

Waste almond and hazelnut nutshells were pretreated with 3, 6 and 9% NaOH and milk of lime under various time and temperature conditions. The XRD analysis results indicated a rise in the crystallinity index with alkaline pretreatment. The observed crystal phase was identified as cellulose I, while the presence of calcite was found in both waste nutshell samples after milk-of-lime treatment. According to the FTIR analysis, the unwanted constituents of the lignocellulosic materials, such as lignin, hemicellulose and pectin were removed with pretreatment, although not in their entirety. SEM analysis displayed a change in the waste nutshell morphology with pretreatment, where the surface became rougher due to the deposition of different sodium and calcium phases. This roughness is beneficial since it promotes better adhesion, which is a key for better composite properties. Surface free energies for both waste nutshell samples as well as the adhesion parameters (interfacial free energy, work of adhesion and spreading coefficient) for binary systems comprised of pretreated nutshell as the particulate and different geopolymer samples as the inorganic matrix were calculated. For both waste nutshells, pretreatment with 6% NaOH for 2.5 h at 80 °C resulted in the formation of a particulate biocomposite with the best adhesion properties. However, it should be noted that obtaining a biocomposite

with suitable properties for practical applications depends on many different preparation factors. The results presented in this work serve solely as guidelines for selecting the optimal pretreatment conditions for waste nutshells as well as the best type of inorganic geopolymer matrix. Accordingly, the study of the most promising biocomposite candidates is the subsequent step and the aim of future work.

Author Contributions: Conceptualization, F.B.; methodology, F.B.; formal analysis, F.B. and K.M.; writing—original draft preparation, F.B.; writing—review and editing, K.M. and S.K.; supervision, S.K. All authors have read and agreed to the published version of the manuscript.

Funding: This research was funded by Operational Programme Competitiveness and Cohesion 2014–2020, European Structural and Investment Funds (grant number KK.011.1.02.0299). The APC was funded by the Operational Programme Competitiveness and Cohesion project “Acoustic incombustible panel” (number KK.011.1.02.0299).

Data Availability Statement: Data are contained within the article.

Acknowledgments: The aegis of the University of Zagreb is gratefully acknowledged alongside the Operational Programme Competitiveness and Cohesion 2014–2020.

Conflicts of Interest: The authors declare no conflicts of interest.

References

1. He, K.; Zhang, J.; Zeng, Y. Knowledge domain and emerging trends of agricultural waste management in the field of social science: A scientometric review. *Sci. Total Environ.* **2019**, *670*, 236–244. [CrossRef]
2. Sinka, M.; Korjakins, A.; Bajare, D.; Zimele, Z.; Sahmenko, G. Bio-based construction panels for low carbon development. *Energy Procedia* **2018**, *147*, 220–226. [CrossRef]
3. Jannat, N.; Al-Mufti, R.L.; Hussein, A.; Abdullah, B.; Catgrave, A. Utilisation of nut shell wastes in brick, mortar and concrete: A review. *Constr. Build. Mater.* **2021**, *293*, 123546. [CrossRef]
4. Demirbas, A. Calculation of higher heating values of biomass fuels. *Fuel* **1997**, *76*, 431–434. [CrossRef]
5. Sujatha, A.; Balakrishnan, S.D. Properties of coconut shell aggregate concrete: A review. *Adv. Civil Eng.* **2020**, *83*, 759–769.
6. Huang, G.; Lapsley, K. Almonds. In *Integrated Processing Technologies for Food and Agricultural By-Products*, 1st ed.; Pan, Z., Zhang, R., Zicari, S., Eds.; Academic Press: London, UK, 2019; pp. 373–390. [CrossRef]
7. Demirbas, A. Fuel characteristics of olive husk and walnut, hazelnut, sunflower, and almond shells. *Energy Sources* **2002**, *24*, 215–221. [CrossRef]
8. Yalchi, T. Determination of digestibility of almond hull in sheep. *Afr. J. Biotechnol.* **2010**, *10*, 3022–3026. [CrossRef]
9. Aktas, T.; Thy, P.; Williams, R.B.; McCaffrey, Z.; Khatami, R.; Jenkins, B.M. Characterization of almond processing residues from the Central Valley of California for thermal conversion. *Fuel Process. Technol.* **2015**, *140*, 132–147. [CrossRef]
10. Messaoudi, Y.; Smichi, N.; Bouachir, F.; Gargouri, M. Fractionation and biotransformation of lignocelluloses-based wastes for bioethanol, xylose and vanillin production. *Waste Biomass Valoriz.* **2017**, *10*, 357–367. [CrossRef]
11. McCaffrey, Z.; Torres, L.; Flynn, S.; Cao, T.; Chiou, B.S.; Klamczynski, A.; Glenn, G.; Orts, M.J. Recycled polypropylene-polyethylene torrefied almond shell biocomposites. *Ind. Crops Prod.* **2018**, *25*, 425–432. [CrossRef]
12. Al-Ajji, M.A.; Al-Ghouti, M.A. Novel insights into the nano-adsorption mechanisms of crystal violet using nano-hazelnut shell from aqueous solution. *J. Water Process Eng.* **2021**, *44*, 102354. [CrossRef]
13. Contini, M.; Baccelloni, S.; Massantini, R.; Anelli, G. Extraction of natural antioxidants from hazelnut (*Corylus avellana* L.) shell and skin wastes by long maceration at room temperature. *Food Chem.* **2008**, *110*, 659–669. [CrossRef]
14. Çam, A.S. Characterization of Clay Brick Materials Produced with Red Mud and Nut Shell Wastes for Building Applications. Master’s Thesis, Izmir Katip Çelebi University, Izmir, Turkey, 2017. Available online: <http://hdl.handle.net/11469/683> (accessed on 17 July 2023).
15. Demirbas, A.; Aslan, A. Effects of ground hazelnut shell, wood, and tea waste on the mechanical properties of cement. *Cem. Concr. Res.* **1998**, *28*, 1101–1104. [CrossRef]
16. Brleković, F.; Fiolčić, T.; Šipušić, J. Sustainable insulating composite from almond shell. In Proceedings of the 2nd International Conference Construction Materials for a Sustainable Future, CoMS 2020/21, Bled, Slovenia, 20–21 April 2021; Šajna, A., Legat, A., Jordan, S., Horvat, P., Kemperle, E., Dolenc, S., Ljubešek, M., Michelizza, M., Eds.; Slovenian National Building and Civil Engineering Institute: Ljubljana, Slovenia, 2020; pp. 32–39.
17. Abdelmouleh, M.; Boufi, S.; Belgacem, M.N.; Dufresne, A. Short natural-fibre reinforced polyethylene and natural rubber composites: Effect of silane coupling agents and fibres loading. *Compos. Sci. Technol.* **2007**, *67*, 1627–1639. [CrossRef]
18. Bychkov, A.L.; Podgorbunskikh, E.M.; Ryabchikova, E.I.; Lomovsky, O.I. The role of mechanical action in the process of the thermomechanical isolation of lignin. *Cellulose* **2018**, *25*, 338–347. [CrossRef]

19. Perez-Rodriguez, N.; Garcia-Bernet, D.; Dominguez, J.M. Faster methane production after sequential extrusion and enzymatic hydrolysis of vine trimming shoots. *Environ. Chem. Lett.* **2017**, *16*, 295–299. [[CrossRef](#)]
20. Contreras-Hernández, M.G.; Ochoa-Martínez, L.A.; Rutiaga-Quiñones, J.G.; Rocha-Guzmán, N.E.; Lara-Ceniceros, T.E.; Contreras-Esquivel, J.C.; Barragán, L.P.; Rutiaga-Quiñones, O.M. Effect of ultrasound pre-treatment on the physicochemical composition of *Agave durangensis* leaves and potential enzyme production. *Bioresour. Technol.* **2018**, *249*, 439–446. [[CrossRef](#)]
21. Kumar, A.K.; Sharma, S. Recent updates on different methods of pretreatment of lignocellulosic feedstocks: A review. *Bioresour. Bioprocess.* **2017**, *4*, 7. [[CrossRef](#)]
22. Hasan, A.; Rabbi, M.S.; Billah, M.M.D. Making the lignocellulosic fibers chemically compatible for composite: A comprehensive review. *Clean. Mater.* **2022**, *4*, 100078. [[CrossRef](#)]
23. Jedrzejczyk, M.; Soszka, E.; Czapnik, M.; Ruppert, A.M.; Grams, J. Physical and chemical pretreatment of lignocellulosic biomass. In *Second and Third Generation of Feedstocks: The Evolution of Biofuels*, 1st ed.; Basile, A., Dalena, F., Eds.; Elsevier: Amsterdam, The Netherlands, 2019; pp. 143–196.
24. Kriven, W.M. 5.9 Geopolymer-based composites. In *Comprehensive Composite Materials II*; Beaumont, P.W.R., Zweben, C.H., Eds.; Academic Press: Oxford, UK, 2018; Volume 5, pp. 269–280.
25. Davidovits, J. *Geopolymer Chemistry and Applications*, 5th ed.; Institut Geopolymere: Saint-Quentin, France, 2020; pp. 3–338.
26. Alawi, A.; Milad, A.; Barbieri, D.; Alosta, M.; Alaneme, G.U.; Imran Latif, Q.B.A. Eco-Friendly geopolymer composites prepared from agro-industrial wastes: A state-of-the-art review. *CivilEng* **2023**, *4*, 433–453. [[CrossRef](#)]
27. Mahmood, A.; Noman, M.T.; Pechočiková, M.; Amor, N.; Petru, M.; Abdelkader, M.; Militký, J.; Sozcu, S.; Hassan, S.Z.U. Geopolymers and fiber-reinforced concrete composites in civil engineering. *Polymers* **2021**, *13*, 2099. [[CrossRef](#)]
28. Fityk Curve Fitting and Data Analysis. Available online: <https://fityk.nieto.pl/> (accessed on 25 February 2023).
29. Pustak, A.; Denac, M.; Leskovic, M.; Švab, I.; Musil, V.; Šmit, I. Structure and morphology of silica-reinforced polypropylene composites modified with m-EPR copolymers. *J. Polym. Res.* **2016**, *23*, 37. [[CrossRef](#)]
30. Chen, H.; Yu, Y.; Zhong, T.; Wu, Y. Effect of alkali treatment on microstructure and mechanical properties of individual bamboo fibers. *Cellulose* **2016**, *24*, 333–347. [[CrossRef](#)]
31. Sun, Q.; Foston, M.; Sawada, D.; Pingali, S.V.; O'Neill, H.M.; Li, H.; Wyman, C.E.; Langan, P.; Pu, Y.; Ragauskas, A.J. Comparison of changes in cellulose ultrastructure during different pretreatments of poplar. *Cellulose* **2014**, *21*, 2419–2431. [[CrossRef](#)]
32. Ferreira, S.R.; Silva, F.D.A.; Lima, P.R.L.; Toledo Filho, R.D. Effect of fiber treatments on the sisal fiber properties and fiber-matrix bond in cement based systems. *Constr. Build. Mater.* **2015**, *101*, 730–740. [[CrossRef](#)]
33. Sanchez-Echeverri, L.A.; Medina-Perilla, J.A.; Ganjian, E. Nonconventional Ca(OH)₂ Treatment of Bamboo for the Reinforcement of Cement Composites. *Materials* **2020**, *13*, 1892. [[CrossRef](#)]
34. Le Troedec, M.; Sedan, D.; Peyratout, C.; Bonnet, J.P.; Smith, A.; Guinebretiere, R.; Gloaguen, V.; Krausz, P. Influence of various chemical treatments on the composition and structure of hemp fibres. *Compos. Part A Appl. Sci. Manuf.* **2008**, *39*, 514–522. [[CrossRef](#)]
35. Rahman, A.; Ulven, C.A.; Johnson, M.A.; Durant, C.; Hossain, K.G. Pretreatment of Wheat Bran for Suitable Reinforcement in Biocomposites. *J. Renew. Mater.* **2017**, *5*, 62–73. [[CrossRef](#)]
36. Barreto, A.C.H.; Rosa, D.S.; Fehine, P.B.A.; Mazzetto, S.E. Properties of sisal fibers treated by alkali solution and their application into cardanol-based biocomposites. *Compos. Part A Appl. Sci. Manuf.* **2011**, *42*, 492–500. [[CrossRef](#)]
37. Zhang, F.-D.; Xu, C.; Li, M.-Y.; Chen, X.-D. Identification of *Dalbergia cochinchinensis* (CITES Appendix II) from other three *Dalbergia* species using FT-IR and 2D correlation IR spectroscopy. *Wood Sci. Technol.* **2016**, *50*, 693–704. [[CrossRef](#)]
38. Javier-Astete, R.; Jimenez-Davalos, J.; Zolla, G. Determination of hemicellulose, cellulose, holocellulose and lignin content using FTIR in *Calycophyllum spruceanum* (Benth.) K. Schum. and *Guazuma crinita* Lam. *PLoS ONE* **2021**, *16*, e0256559. [[CrossRef](#)] [[PubMed](#)]
39. Li, X.; Liu, Y.; Hao, J.; Wang, W. Study of Almond Shell Characteristics. *Materials* **2018**, *11*, 1782. [[CrossRef](#)] [[PubMed](#)]

Disclaimer/Publisher's Note: The statements, opinions and data contained in all publications are solely those of the individual author(s) and contributor(s) and not of MDPI and/or the editor(s). MDPI and/or the editor(s) disclaim responsibility for any injury to people or property resulting from any ideas, methods, instructions or products referred to in the content.